

Integration within Polygonal Finite Elements

Gautam Dasgupta, M.ASCE¹

Abstract: Engineering mechanics formulations of aerospace industry problems overwhelmingly rely upon spatial averaging techniques. Crucial applications in the area of dynamic response analysis and stochastic estimation of material degradation can be cited as important cases. Integration procedures on finite domains underlie physically acceptable averaging processes. Unlike one-dimensional cases, integrals within arbitrary areas and volumes cannot be approximated by a Gaussian form of numerical quadrature. Here the divergence theorem is applied once and twice, respectively, for polygonal and polyhedral integration domains, to construct integrals on boundary wireframes. The sum of Gaussian quadrature values on linear segments of the wireframe yields the final result of numerical integration on a finite element.

DOI: 10.1061/(ASCE)0893-1321(2003)16:1(9)

CE Database keywords: Finite elements; Boundary element method; Polygons; Computation.

Introduction

Averaging process is the most frequently employed concept in computational techniques pertaining to the aerospace industry. In probabilistic estimations, and in spatially discretized approximations, e.g., finite- and boundary-element methods, evaluation of integrals over arbitrary-shaped regions becomes the pivotal task that underlies the selected averaging procedure.

Numerical integration methods extensively employ the Gaussian quadrature technique that was originally designed for one-dimensional cases. Its order can be set to achieve a predetermined numerical accuracy goal. The procedure naturally extends to two- and three-dimensional rectangular domains according to the notion of the Cartesian product. This guarantees a prescribed accuracy when the quadrature is carried out within areas and volumes that are bounded by orthogonal lines and planes, respectively.

As illustrated in Fig. 1(a), an affine transformation (Rogers and Adams 1990) produces a nonorthogonal skewed system of coordinates from a rectangular domain. All affine maps preserve the accuracy of Gaussian quadratures. There is no computational difficulty in evaluating any domain integral numerically when the two- and three-dimensional regions are bounded, respectively, by systems of parallel lines and parallel planes.

All shapes that result from affine transformations of generalized rectangles in \mathcal{R}^n constitute the class of brick domains. Their boundaries are linear manifolds in \mathcal{R}^{n-1} (Aleksandrov 1960). In general, the Gaussian quadrature in its original form can be implemented in n -dimensional space \mathcal{R}^n if the domain is a "brick" in a skewed coordinate system. The numerical integral results from the sum of Gaussian quadratures on one-dimensional segments situated within the brick. For nonparallelogram quadri-

laterals there is no consistent procedure to select the sampling points to implement a Gaussian quadrature on the entire element.

Fig. 1(b) shows the image of a square after a perspective transformation (Rogers and Adams 1990). The opposite sides, in general, may not remain parallel in such a shape even though the straight boundary segments are preserved. Such quadrilateral elements are very frequent in finite-element modeling.

Special integration schemes, e.g., reduced integration, over quadrilaterals have been successfully developed (Hughes 1987) and are widely used in commercial programs. There is no methodical way to design such approximate integration schemes for polygons with more than four sides.

An attempt to distribute the sampling points according to the governing perspective transformation fails to assure the error order germane to the quadrature formula. The reason can be traced to the crowding of quadrature points in Fig. 1(b). This numerical computational difficulty, which persists in all nonparallelogram polygonal finite elements, is circumvented in this paper. The domain integral is converted to a sum of line integrals by the application of the divergence theorem.

Specific Applications

Convention for Coordinates

In practical finite-element calculations a node i is designated in the x - y or x - y - z frame as (x_i, y_i) or (x_i, y_i, z_i) , respectively. In tensor-based formulations the indicial notation x_1 - x_2 and x_1 - x_2 - x_3 are used. In the following sections the coordinate notation x - y or x - y - z and x_1 - x_2 or x_1 - x_2 - x_3 is explicitly clarified to avoid any possible confusion.

Needs for High-Accuracy Integration Methods

This paper has been motivated by numerical methods related to stochastic finite-element and stochastic boundary-element formulations (Dasgupta 1992). The secondary effects of material and geometrical randomness require that all lower-order conditions be met as accurately as possible; e.g., stochastic finite elements,

¹Dept. of Civil Engineering and Engineering Mechanics, School of Engineering and Applied Science, Columbia Univ., 500 West 120 St., New York, NY 10027. E-mail: dasgupta@columbia.edu

Note. Discussion open until June 1, 2003. Separate discussions must be submitted for individual papers. To extend the closing date by one month, a written request must be filed with the ASCE Managing Editor. The manuscript for this paper was submitted for review and possible publication on February 22, 2002; approved on June 10, 2002. This paper is part of the *Journal of Aerospace Engineering*, Vol. 16, No. 1, January 1, 2003. ©ASCE, ISSN 0893-1321/2003/1-9-18/\$18.00.

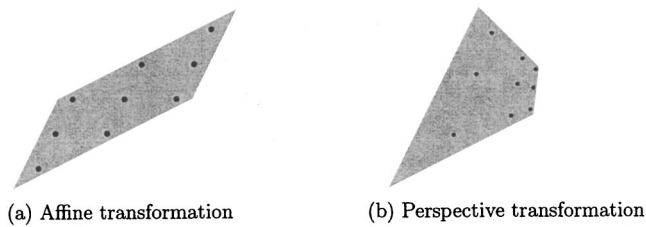


Fig. 1. Transformed quadrature points on a square

which do not use stochastic shape functions and fail to satisfy equilibrium conditions, are not suitable for high-precision reliability analysis.

Integration schemes based on weighted residuals are prone to instability since the accuracy goal cannot be controlled. In deterministic cases the underlying averaging process may be inconsistent, which was stated in Strang and Fix (1973) as a *variational crime*. In stochastic differential equation literature (Keller 1964; Keller and McKean 1973), such averaging processes are termed *dishonest*, (Molyneux 1968).

Here the examples adequately illustrate the effectiveness of the integration procedure developed for polygons of arbitrary shapes. First, the probability integral over a triangle is evaluated. Next, a stiffness matrix of a quadrilateral element is illustrated. This is more accurate than the prevalent isoparametric formulation with heuristic integration schemes (Zienkiewicz and Taylor 1977).

Component Failure Statistics

In complex engineering systems, analysts cannot ignore the randomness in material properties and uncertainty in geometry that are frequently encountered in the aerospace industry. The vital components are rated during quality control inspections according to reliability indices calculated from the average probability density functions that model failure. This entails the evaluation of an integral of the joint probability frequency function $f_{xyz}(x,y,z)$ over the volume Ω of the component.

In general, the Ω shape-class that accounts for the engine components and structural parts of the aircraft body is very irregular in two- and three-dimensional geometry. Straightforward Gaussian quadrature in those higher dimensions will yield inconsistent and unreliable failure probabilities. Such an averaging process defeats the purpose of secondary considerations of material and geometrical randomness.

In this paper, the divergence theorem is implemented to convert the volume integral on Ω to a surface integral on its boundary Γ . In finite- and boundary-element procedures, surfaces like Γ are usually approximated to collections of polygons enclosed by lines Λ . In the proposed development, on each polygon the divergence theorem is applied once more. This confines the integration to the boundary lines Λ of the aforementioned polygons.

The Gaussian quadrature on each linear (one-dimensional) segment of Λ can be executed to meet any preassigned accuracy goal. The sum of the numerical quadrature results yields the integral on the volume Ω . This accurate procedure to evaluate integrals on arbitrary shapes is recommended to formulate numerical techniques to aid effective inspection and safe design. A Gaussian quadrature on a segment of Λ is illustrated in Appendix I.

Finite-Element System Matrices

The nondimensional finite-element system matrices are averages of energy densities. Elements of stiffness, mass, and thermal conductivity matrices represent averages of strain, kinetic, and heat energies, respectively. A nondimensional domain integral in a boundary-element formulation results from averaging an intensive quantity. To address these problems, a numerical scheme is developed here to approximate integrals over arbitrary domains bounded by straight lines and plane faces. The divergence theorem furnishes the mathematical basis for converting the energy density integration to one-dimensional line integrals that can be evaluated by a Gaussian quadrature (see Appendix I). Because of its popularity the finite-element method is selected to outline the proposed formulation.

In the finite-element method, the local stiffness $[k]$ and mass $[m]$ matrices are the integrals of the appropriate energy density functions within the discrete domain Ω . Considerable research has been directed to devise integration schemes on two- and three-dimensional elements (MacNeal 1994). The solution space is approximated by a set of shape functions that are used to construct the strain energy density expressions in the stiffness matrix formulation. For example, in a plane-strain element, the strain-displacement transformation matrix $[B]$ is determined in terms of shape function derivatives. The associated constitutive matrix, $[D]$, is then used to express the strain energy density influence matrix $[U]$ (Zienkiewicz and Taylor 2000) in the form.

$$[U]=[B]^T[D][B] \quad (1)$$

The stiffness matrix, $[K]$, is evaluated as the domain integral

$$[K]=\int_{\Omega}([B]^T[D][B])d\Omega; \quad \Omega:\text{element volume} \quad (2)$$

of the strain energy density distribution $[U]$ within the element volume Ω .

The power of the finite-element method is evidenced by the ease of covering a body of arbitrary shape with regions of relatively simple geometry. In two- and three-dimensional problems, the typical elements are popular convex polygons and polyhedra with straight edges. A variety of shape functions are available in the literature, e.g., for two-dimensional plane stress and plane-strain triangles and quadrilaterals, and special purpose three-dimensional plates and shell elements. Almost all currently available commercial programs evaluate the domain integrals within those finite elements according to numerical quadrature schemes with varied degrees of accuracies.

Beyond axisymmetric cases, elements with general curved edges require complicated mathematical transformations (Wachspress 1971) for the generation of the appropriate shape functions. Also, integrations of energy densities within those elements are quite involved. All necessary formulation and development is best carried out with the aid of a computer algebra system, e.g., *Mathematica* (Wolfram 1997), rather than under a conventional Fortran, C, or C++ procedural environment.

On three-node triangular elements the interpolants are linear functions in the coordinate variables. Their spatial derivatives, which enter in $[B]$, are constants. Standard textbooks furnish close-form expressions for $[B]$ (e.g., Reddy 1984, p. 269, for such details). The consistent mass matrices, $[M]$, are quadratic in coordinate variables. The integration of any polynomial in triangular domains can be carried out exactly by quadrature. This observation furnished a crucial advantage in the early development of the

finite-element method, as pointed out in Strang and Fix (1973, p. 181).

A considerable amount of research has been performed to attain perfect results of domain integration for plane quadrilateral elements when numerical quadrature techniques are employed (§5.5 in Bathe 1996). The accuracy of a selected quadrature strategy is indicated by compliance with the *patch-test* proposed by Irons (Irons and Razzaque 1972). This exercise was undertaken for quadrilateral elements as reported in Dasgupta (2000).

The overall error in a finite-element calculation can be reduced by not relying so heavily on artificial tessellation (i.e., discretization with subparts), which requires the deployment of elements with large numbers of sides. Wachspress (1975) developed an elegant systematic procedure to yield shape functions for convex polygons of arbitrary numbers of sides. The energy density, which is described above as $[B]^T[D][B]$, can be obtained in closed algebraic form in terms of rational polynomials. However, a direct Gaussian quadrature scheme to numerically evaluate the domain integral, $\int_{\Omega}([B]^T[D][B])$, on n -sided polygons cannot be constructed to yield the exact results, even on convex quadrilaterals. This shortcoming is eliminated here.

The objective of the present formulation is to devise an integration method that will be applicable for all n -sided polygons. The divergence theorem of multivariable calculus furnishes the foundation of the proposed formulation. The domain integrals are converted to boundary integrals and are evaluated on straight-line segments according to desired numerical quadrature formulas.

The high-accuracy integration method is meaningful only when the shape functions are the very best. One does not face any difficulty with triangular elements where the exact shape functions are available and the quadrature formulas are also exact. A concise description, which appears in Zienkiewicz and Taylor (1977), is summarized next.

Summation over Simplex Domains

Here the assumptions are that the two-dimensional finite elements have straight-line boundaries and that the three-dimensional ones are bounded by planes. Triangles and tetrahedrons are the corresponding simplex shapes in two and three dimensions, respectively (Aleksandrov 1960).

For the purpose of computing the exact integral of a function f :

$$\mathcal{I} = \int_{\Omega} f d\Omega; \quad \Omega: \text{element domain} \quad (3)$$

observe that \mathcal{I} can be calculated as a sum of integrals evaluated over simplex divisions Δ_i :

$$\Omega = \cup_i \Delta_i; \Delta_i \text{ completely covers } \Omega \quad (4)$$

Δ_i =triangle or=tetrahedron for two- or three-dimensional domains, respectively. Now Eq. (3) can be rewritten as

$$\mathcal{I} = \int_{\Omega} f d\Omega = \sum_i \int_{\Delta_i} f d\Delta_i \quad (5)$$

In the interest of describing the integration scheme, it suffices to set up a computer program to work on simplex regions. However, tessellation into simplex regions invites additional integration segments. For example, a hexagonal figure (Fig. 2), when triangulated, will need 12 line segments, which will double the computing time.

As a general rule, tessellation into simplex regions is not necessary for the purpose of domain integration and should be avoided.

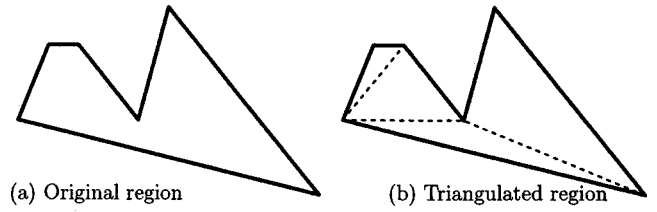


Fig. 2. Nonessential triangulation

In the following section, in the interest of generality, integration within regions bounded by planes and straight lines, as in two- and three-dimensions respectively, is presented. The regions need not be convex; a reentrant corner for a concave region, such as star-polytopes (Coxeter 1960), does not pose any additional difficulty.

Volume Integrals

Indicial Notation

The conventional (x, y, z) coordinate system rewritten in the indicial form as (x_1, x_2, x_3) facilitates the development because the formulation is based on vector algebra.

Quadrature within Polyhedra

Let the volume V , in a coordinate system (x_1, x_2, x_3) , be enclosed by the surface S . Let the unit vectors along the coordinate directions x_1, x_2, x_3 be indicated by $\hat{i}_1, \hat{i}_2, \hat{i}_3$, respectively.

Consider a generic (scalar) function $u(x_1, x_2, x_3)$ whose integral in V is to be evaluated. We will construct a vector $\hat{\Phi}(x_1, x_2, x_3)$ that will satisfy

$$u = \text{div } \hat{\Phi} \quad (6a)$$

where

$$\hat{\Phi} = \phi_1 \hat{i}_1 + \phi_2 \hat{i}_2 + \phi_3 \hat{i}_3 \quad (6b)$$

The components ϕ_1, ϕ_2, ϕ_3 are assumed to be integrable everywhere within the volume V .

The boundary surface S of the volume V is composed of k plane polygonal faces $S_i, i=1, k$. The divergence theorem in terms of a function $\hat{\Phi}(S)$, which is defined only on the boundary S according to a dot product \odot , leads to

$$\int_V u(x_1, x_2, x_3) dV = \int_S \hat{\Phi} \odot \hat{n} dS \quad (7a)$$

$$\int_V \text{div } \hat{\Phi} dV = \oint_S \hat{\Phi} \odot \hat{n} dS = \oint_S (\phi_1 n_1 + \phi_2 n_2 + \phi_3 n_3) dS \quad (7b)$$

$$\text{outward normal on } S: \hat{n} = n_1 \hat{i}_1 + n_2 \hat{i}_2 + n_3 \hat{i}_3 \quad (7c)$$

In order to satisfy $u = \text{div } \hat{\Phi}$, assume

$$\phi_2 = \phi_3 = 0, \quad (8a)$$

and

$$\phi_1(x_1, x_2, x_3) = \int u(x_1, x_2, x_3) dx_1 + c(x_2, x_3) \quad (8b)$$

$$c: \text{arbitrary function independent of } x_1 \quad (8c)$$

The determination of the arbitrary function $c(x_2, x_3)$ in Eq. (8b) is a crucial step in computing the volume integral in Eq. (7a).

Now the volume integral in Eq. (7a) becomes a surface integral as follows:

$$\int_V u(x_1, x_2, x_3) dV = \int_S \phi_1 n_1 dS \quad (9a)$$

$$= \int_S \left(\int u(x_1, x_2, x_3) dx_1 \right) n_1 dS + \int_S c(x_2, x_3) n_1 dS \quad (9b)$$

$$= \int_S \left(\int u(x_1, x_2, x_3) dx_1 \right) dS^1 + \int_S c(x_2, x_3) dS^1 \quad (9c)$$

$$dS^j = n_j dS: \text{surface element projected on a plane } \perp \hat{i}_j \quad (9d)$$

The arbitrariness in Eq. (9c) must be resolved by establishing the zero effect of the arbitrary function c that appeared during indefinite integration in Eq. (8b). Let us consider the second integral in Eq. (9b), which contains that c . Let us view the surface S with the line of sight (or rays) along \hat{i}_1 . For each element dS^1 in front of the observer, there is the $-dS^1$ on the other side. Both elements will have identical $c(x_2, x_3)$ value since c does not depend on x_1 . Thus the net contribution of the pair of $\pm dS^1$ is zero. Hence, the integral of c on the entire projected surface is zero:

$$\int_S c(x_2, x_3) dS^1 = 0 \quad (10)$$

This allows us to write Eq. (9b) as

$$\int_V u(x_1, x_2, x_3) dV = \int_S \left(\int u(x_1, x_2, x_3) dx_1 \right) n_1 dS \quad (11)$$

The boundary integral can be evaluated on the individual polygon S_j that defines the surface S . The volume integral in Eq. (9a) thus reduces to a sum that can be computed on individual polygon S_j :

$$\int_V u(x_1, x_2, x_3) dV = \sum_{j=1}^k \int_{S_j} \int u(x_1, x_2, x_3) dx_1 dS_j^1 \quad (12)$$

In this presentation the indefinite integral

$$\int u(x_1, x_2, x_3) dx_1 = \varphi(x_1, x_2, x_3) \quad (13)$$

is analytically evaluated. In general, a computer mathematics environment, e.g., *Mathematica* (Wolfram 1997), becomes useful. The same result $\varphi(x_1, x_2, x_3)$ will be used in all polygonal surface parts dS_j .

The projected area dS_j^1 is perpendicular to \hat{i}_1 and lies on the (x_2, x_3) plane. The equation of the plane face dS_j can be expressed as

$$x_1 = x_1^{(j)}(x_2, x_3) = \alpha_1^{(j)} + \alpha_2^{(j)} x_2 + \alpha_3^{(j)} x_3 \quad (14)$$

Thus the right-hand side of Eq. (12) can be simplified to be

$$\int_V u(x_1, x_2, x_3) dV = \sum_{j=1}^k \int_{S_j} \varphi(x_1^{(j)}(x_2, x_3), x_2, x_3) dS_j^1 \quad (15a)$$

$$= \sum_{j=1}^k \int_{S_j} \varphi^{(j)}(x_2, x_3) dS_j^1 \quad (15b)$$

Let us examine a generic term under the summation $\int_{S_j} \varphi^{(j)}(x_2, x_3) dS_j^1$. The surface subset S_j^1 is a polygon in the (x_2, x_3)

region; on this a two-dimensional entity, a function $\varphi^{(j)}$ of (x_2, x_3) , is to be integrated. We will formulate here a method that can be repeatedly used for all boundary polygons $j=1, k$.

The computation of the volume integral of Eq. (7a) essentially rests on a procedure to integrate an arbitrary function within a polygon [Eq. (15b)]. This procedure is elaborated in the following section.

Two-Dimensional Cases

Indicial Notation

The general development is carried out in the indicial form with the (x_1, x_2) coordinate system. As evidenced in the previous section, this is better suited than the conventional (x, y) frame.

Quadrature within Polygon

The three-dimensional element in the previous section is assumed to be enclosed by a surface that is a collection of plane-face polygons. A typical surface "patch," which is a κ -sided polygon, does not have to be convex. In this integration procedure concavity does not pose any additional problem.

The steps to evaluate the integral of a function $v(x_1, x_2)$ within a polygon Ω with a circumference Γ are close to the one presented to evaluate the volume integral. In order to implement the divergence theorem, a vector function $\hat{\Psi}$ is defined to be

$$\int_{\Omega} v(x_1, x_2) d\Omega = \int_{\Gamma} \hat{\Psi} \odot \hat{n} d\Gamma \quad (16a)$$

$$\hat{\Psi} = \Psi_1 \hat{i}_1 + \Psi_2 \hat{i}_2; \quad \hat{n} = n_1 \hat{i}_1 + n_2 \hat{i}_2 \quad (16b)$$

furthermore,

$$\Psi_1(x_1, x_2) = \int v(x_1, x_2) dx_1 + c(x_2); c: \text{arbitrary} \quad (16c)$$

and

$$\Psi_2(x_1, x_2) = 0 \quad (16d)$$

Almost all v related to mathematical physics can be integrated in one variable, as in Eq. (16c), by a computer mathematics environment, such as *Mathematica* (Wolfram 1997).

The construction of the vector function $\Psi(x_1, x_2)$ is very similar to that in Eqs. (6a) and (8b) for the three-dimensional case. Here we will explicitly show that

$$\int_{\Gamma} c(x_2) \hat{i}_1 \odot \hat{n} d\Gamma = \quad (17a)$$

$$\int_{\Gamma} c(x_2) n_1 d\Gamma = 0 \quad (17b)$$

We shall consider Γ to define a convex polygon. For the purpose of this theoretical proof of Eq. (17b), any concave polygon in question can be tessellated into convex ones (de Berg et al. 2000). On each convex part the zero condition will prevail.

In Eq. (17b) n_1 is the cosine of the angle between the outward normal on Γ and x_1 (Fig. 3). It is then convenient to divide Γ into two parts, Γ^+, Γ^- , on which n_1 is positive and negative, respectively. The positive part Γ^+ is from the bottom-most point to the top-most, and Γ^- is from the top to the bottom. Fig. 3 facilitates viewing by showing Γ^+ thicker than Γ^- .

At $x_2 = x_2^{(0)}$ let us consider two differential elements $d\Gamma^+$ and $d\Gamma^-$ bounded between two horizontal lines, shown with dashes in

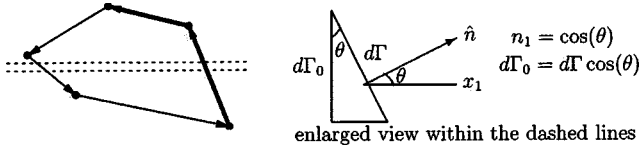


Fig. 3. Path element in contour integral

Fig. 3. In the integrand of Eq. (17b) $n_1 d\Gamma$ value will be $\pm d\Gamma_o$ on $d\Gamma^+$ and $d\Gamma^-$, respectively. The values of $c(x_2)$ within the integral in Eq. (17b) remain the same on these two paths, and are equal to $c(x_2^{(0)})$. Hence,

$$n_1 c(x_2) d\Gamma = n_1 c(x_2^{(0)}) d\Gamma^+ + n_1 c(x_2^{(0)}) d\Gamma^- = c(x_2^{(0)}) d\Gamma_o + c(x_2^{(0)}) (-d\Gamma_o) = 0 \quad (18)$$

The entire contour in Eq. (17b) can be divided into such differential segments $d\Gamma$ (e.g., $d\Gamma^+$ and $d\Gamma^-$) and on each the net contribution of $c(x_2) d\Gamma$ will be zero. Hence their sum, which is represented as an integral, in Eq. (17b) is zero. The arbitrary function c in Eq. (16c) is then inconsequential. Any indefinite integral—

$$\Psi_1(x_1, x_2) = \int v(x_1, x_2) dx_1 \quad (19)$$

—should suffice.

The integral in Eq. (19) will be evaluated analytically. Closed-form expressions for almost all finite-element-related functions can be obtained when a suitable computer mathematics environment (e.g., *Mathematica*) is employed. The lack of uniqueness of an indefinite integral does not pose a problem, since Eq. (17b) remains valid for all convex subsections of a boundary plane.

The area integral in Eq. (16a) simplifies to

$$\int_{\Omega} v(x_1, x_2) d\Omega = \int_{\Gamma} \Psi_1(x_1, x_2) n_1 d\Gamma \quad (20)$$

The right-hand integral can be calculated by a suitable quadrature on one-dimensional boundary pieces defined as the sides of the polygon Ω .

The perimeter Γ is a collection of straight-line sides Γ_j , $j = 1, \kappa$ for the κ -sided domain Ω . The boundary integral in Eq. (20) can be written as a sum of integrals on the sides of the polygon:

$$\int_{\Omega} v(x_1, x_2) d\Omega = \int_{\Gamma} \Psi_1(x_1, x_2) n_1 d\Gamma = \sum_{j=1}^{\kappa} \int_{\Gamma_j} \Psi_1(x_1, x_2) n_1 d\Gamma \quad (21)$$

A generic term within the summation sign can be further simplified. On a polygonal side j the direction cosine n_1 is a constant $n_1^{(j)}$ and can be expressed in terms of the end-point coordinates. The equation of the side is a linear function in x_2 : $x_1 = x_1^{(j)}(x_2)$. Now,

$$\int_{\Gamma_j} \Psi_1(x_1, x_2) n_1 d\Gamma = \int_{\Gamma_j} \Psi_1(x_1^{(j)}(x_2), x_2) n_1^{(j)} d\Gamma \quad (22)$$

Observe:

$$n_1^{(j)} d\Gamma = dx_2 \quad (23)$$

Let the x_2 end coordinates for the j th side be $x_2^{j\text{-start}}$ and $x_2^{j\text{-end}}$. The left-hand side of Eq. (22) becomes

$$\int_{\Gamma_j} \Psi_1(x_1, x_2) n_1 d\Gamma = \int_{x_2^{j\text{-start}}}^{x_2^{j\text{-end}}} \Psi_1(x_1^{(j)}(x_2), x_2) dx_2 \quad (24)$$

$$= \int_{x_2^{j\text{-start}}}^{x_2^{j\text{-end}}} \mathcal{V}_j(x_2) dx_2 \quad (25)$$

where

$$\mathcal{V}_j(x_2) = \Psi_1(x_1^{(j)}(x_2), x_2) \quad (26)$$

Standard computer mathematics systems provide a fifth-order Gaussian quadrature formula as the default procedure to numerically evaluate one-dimensional integrals such as Eq. (25).

In order to implement the Gaussian quadrature scheme it is more convenient to express Eq. (22) in the parametric form where the integration variable, τ , runs from 0 to 1. This is explained below in terms of a generic function $f = \Psi_1$ of Eq. (24) in the familiar x - y frame. The normal component n_1 is indicated by the familiar direction cosine $\cos(\theta)$.

Numerical Integration Along Polygonal Side

Cartesian Coordinates

Most of the finite-element computer programs are written with (x, y, z) notations rather than in the indicial form that is exclusively devoted for theoretical development. In that spirit the two-dimensional examples are presented here in the (x, y) frame.

Furthermore, the conventional notation to indicate the nodal coordinate is (x_i, y_i) for the finite-element node i . The context for (x_1, x_2, x_3) and (x_i, y_i) are different; hence all confusions are averted in the literature. Here such a tradition will be maintained.

Development of Line Integrals

The generic integral

$$\int_0^l f(x, y) \cos(\theta) dl; \text{ between } (x_1, y_1) \text{ and } (x_2, y_2) \quad (27)$$

is considered in the following parameterized form in terms of the running parameter τ :

$$\tau = \frac{x - x_1}{x_2 - x_1} = \frac{y - y_1}{y_2 - y_1} \quad (28)$$

$$x = x_1 + \tau(x_2 - x_1), \quad y = y_1 + \tau(y_2 - y_1)$$

$$dl = l d\tau \quad (29)$$

Note that θ is the angle between y -axis and \vec{l} ; hence

$$\cos(\theta) = \frac{y_2 - y_1}{l} \quad (30)$$

from Eq. (29):

$$dl \cos(\theta) = (y_2 - y_1) d\tau \quad (31)$$

Now Eq. (27) becomes

$$(y_2 - y_1) \int_0^1 f[x_1 + \tau(x_2 - x_1), y_1 + \tau(y_2 - y_1)] d\tau \quad (32)$$

and the Gaussian quadrature formula can now be directly implemented.

To help develop a computer program, e.g., a fifth-order quadrature, which is necessary in Eq. (32), sampling points and the corresponding weights are included in Appendix I.

Numerical Example

The general strategy is to convert a volume integral to the surface one according to the divergence theorem. The theorem is repeated to transform the surface integrals into contour integrals. It is assumed that the wireframe boundaries of interest are composed of straight-line segments. The one-dimensional integration on a straight-line segment constitutes the numerical engine of the proposed strategy. In the interest of completeness, the paper reviews the one-dimensional quadrature in Appendix I. The one-dimensional closed-form illustration for the example of an area integration is now described.

Area Integration: β -Distribution

In reliability analysis, one needs the integration of typical probability (frequency) density functions. It is possible to evaluate the indefinite integrals of Eq. (21) in closed form for many useful density functions. Let us consider a single variable β -distribution in the x - y coordinates:

$$f_{xy}(x,y) = \frac{(1-x)^{n-1}x^{m-1}}{\beta(m,n)} \quad (33)$$

For simplicity, uniformity along the y -axis is assumed here.

The general indefinite integral $\int f(x,y)dx$ is available in the closed form in term of hypergeometric (higher-order transcendental) functions for all values of m,n (see *Mathematica*, Wolfram 1997). For specific examples when m,n are integers, simple closed-form expressions, which are polynomials in x , can be obtained easily.

Here the example is carried out with $m=3, n=4$ in Eq. (33):

$$f_{xy}(x,y) = \frac{x^2(1-x)^3}{\beta(3,4)} = 60(1-x)^3x^2 \quad (34)$$

This frequency function is integrable in the following closed form:

$$\int f_{xy}(x,y)dx = 60 \left(\frac{x^3}{3} - \frac{3x^4}{4} + \frac{3x^5}{5} - \frac{x^6}{6} \right) \quad (35)$$

An important spot-check is

$$\begin{aligned} \int_0^1 f_{xy}(x,y)dx &= 60 \left(\frac{x^3}{3} - \frac{3x^4}{4} + \frac{3x^5}{5} - \frac{x^6}{6} \right) \Big|_0^1 \\ &= 60 \left(\frac{1}{3} - \frac{3}{4} + \frac{3}{5} - \frac{1}{6} \right) = 1 \end{aligned}$$

In the interest of focusing on the proposed integration scheme, it is sufficient to demonstrate the method on a triangular domain, shown in Fig. 4, connecting the vertices:

$$(x_1, y_1) = (0,0); \quad (x_2, y_2) = \left(\frac{4}{5}, \frac{1}{3} \right); \quad (x_3, y_3) = \left(\frac{2}{3}, \frac{5}{6} \right) \quad (36)$$

The integrand of Eq. (32) is positive throughout the domain. Along the integration path y increases in segments 1 and 2. Hence the integrals along those two segments will contribute positive quantities. The y value decreases along the integration path in segment-3, which yields a negative result in Eq. (32).

The numerical values on segments described in Fig. 4 are

$$\text{segment 1: } (0,0) \text{ to } (4/5, 1/3): \frac{3,392}{21,875} \quad (37a)$$

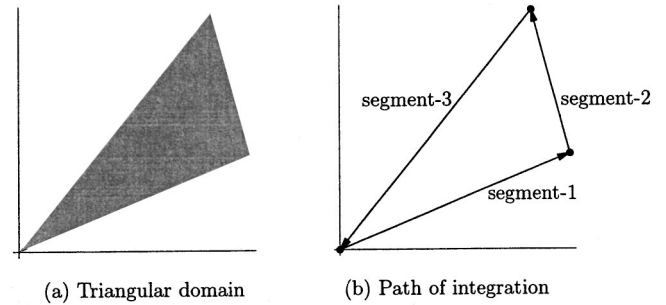


Fig. 4. Example: integration on a triangle

$$\text{segment 2: } (4/5, 1/3) \text{ to } (2/3, 5/6): \frac{7,567,412}{15,946,875} \quad (37b)$$

$$\text{segment 3: } (2/3, 5/6) \text{ to } (0,0): -\frac{4,700}{15,309} \quad (37c)$$

leading to the value $440,944/1,366,875 = 0.322593$, which can be verified by a suitable computer algebra program. The procedure for the first part, whose result appears in Eq. (37a), is elaborated below.

To integrate f_{xy} into Eq. (33), the function f_{xy} in Eq. (34) is first integrated with respect to x leading to the expression in Eq. (35). In Eq. (32), $y_2 = 1/3$, $y_1 = 0$ and $x_1 = 0$, $x_2 = 4/5$ the line integral in this segment-1 becomes

$$\left(\frac{1}{3} - 0 \right) \int_0^1 60 \left(\frac{\left(\frac{4}{5} \tau \right)^3}{3} - \frac{3 \left(\frac{4}{5} \tau \right)^4}{4} + \frac{3 \left(\frac{4}{5} \tau \right)^5}{5} - \frac{\left(\frac{4}{5} \tau \right)^6}{6} \right) d\tau \quad (38a)$$

$$= 20 \int_0^1 \left(\frac{64\tau^3}{375} - \frac{192\tau^4}{625} + \frac{3,072\tau^5}{15,625} - \frac{2,048\tau^6}{46,875} \right) d\tau \quad (38b)$$

$$= \frac{3,392}{21,875} \quad (38c)$$

The final value appears in Eq. (37a).

This one-dimensional integration can be effectively computed according to the Gaussian quadrature formula selected on the basis of the accuracy goal. In most of the numerical codes a fifth-order quadrature is used as the default scheme. The result for Eq. (38b) becomes 0.155063, where the order of the error is 10^{-7} .

Quadrilateral Element

An element of the stiffness matrix for the trapezoid shown in Fig. 5 is computed. The nodes are

$$(-1.125, -0.5), (0.875, -0.5), (0.375, 0.5), (-0.125, 0.5) \quad (39)$$

The following rational finite element shape functions \mathcal{N}_i (Wachspress 1975) guarantees linear distribution on the boundary and reproduce exactly any linear field within the finite-element domain:

$$\mathcal{N}_1 = (0.25 - 0.4x - 0.7y + 0.8xy + 0.4y^2)/(1 - 1.2y) \quad (40a)$$

$$\mathcal{N}_2 = (0.25 + 0.4x - 0.9y - 0.8xy + 0.8y^2)/(1 - 1.2y) \quad (40b)$$

$$\mathcal{N}_3 = (0.25 + 0.4x + 0.1y + 0.8xy - 0.8y^2)/(1 - 1.2y) \quad (40c)$$

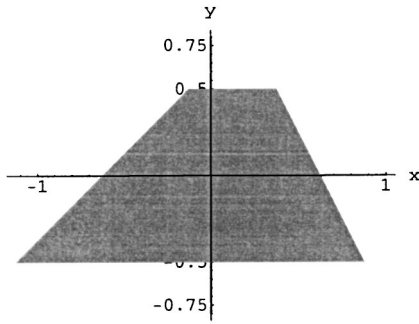


Fig. 5. Two-dimensional element

$$\mathcal{N}_4 = (0.25 - 0.4x + 0.3y - 0.8xy - 0.4y^2) / (1 - 1.2y) \quad (40d)$$

The strain-displacement transformation matrix is in the following form:

$$[b] = \begin{bmatrix} b_{11} & 0 & b_{13} & 0 & b_{15} & 0 & b_{17} & 0 \\ 0 & b_{22} & 0 & b_{24} & 0 & b_{26} & 0 & b_{28} \\ b_{31} & b_{32} & b_{33} & b_{34} & b_{35} & b_{36} & b_{37} & b_{38} \end{bmatrix} \quad (41)$$

Consider a plane stress situation with the shear modulus $\mu=1$ and the Poisson's ratio $\nu=1/3$. The constitutive matrix becomes

$$[d] = \begin{bmatrix} 3 & 1 & 0 \\ 1 & 3 & 0 \\ 0 & 0 & 1 \end{bmatrix} \quad (42)$$

The first element of the stiffness matrix k_{11} in $[k] = \int [b]^T [d] [b] dA$, from Eqs. (41) and (42) becomes

$$k_{11} = \int (3b_{11}^2 + b_{31}^2) dA \quad (43)$$

From the shape function of Eq. (40a):

$$b_{11} = \frac{\partial \mathcal{N}_1}{\partial x} \quad b_{31} = \frac{\partial \mathcal{N}_1}{\partial y} \quad (44)$$

$$= \frac{1.6 - 3.2y}{-4 + 4.8y} = \frac{-0.4 + 0.32x + 0.8y - 0.48y^2}{(1 - 1.2y)^2} \quad (45)$$

$$k_{11} = \int (3b_{11}^2 + b_{31}^2) dA \quad (46a)$$

$$= \int (163.84 - 65.536x + 26.2144x^2 - 950.272y + 131.072xy + 2110.26y^2 - 78.6432xy^2 - 2084.04y^3$$

$$+ 766.771y^4) \frac{dA}{(4 - 4.8y)^4} \quad (46b)$$

$$= 0.861515 \quad (46c)$$

The integral in Eq. (46a) is evaluated as a line integral along the boundary employing Eq. (32). Each term in the integrand of Eq. (46b) was first integrated with respect to x while y was held fixed. The polynomial in x is integrable term by term as needed in Eq. (19).

The aforementioned procedure of numerical integration is recommended in high accuracy finite-element computations.

To facilitate code development and verification with a benchmark example, the full stiffness table is presented in Table 1.

The fifth-order Gaussian quadrature formula, which is the default approximation in *Mathematica*, is used in the aforementioned example. The integration points and the corresponding weights are read from the table provided in Appendix I.

The computer mathematics environment *Mathematica* (version 4.1) printed "10.9167 Second" when it calculated those 64 stiffness values in Table 1 independently in a 500 MHz Macintosh computer.

A typical indefinite integral, which is necessary to implement the divergence theorem, [Eq. (19)], can be calculated using a computer mathematics environment.

The following two *Mathematica* results are furnished to verify the numerics during the code development:

$$\int 3b_{11}^2 + b_{31}^2 dx = \int \frac{3(-1.6 + 3.2y)^2}{(4 - 4.8y)^2} + \frac{(-6.4 + 5.12x + 12.8y - 7.68y^2)^2}{(4 - 4.8y)^4} dx = \frac{p_1(x, y)}{q_1(x, y)},$$

where

$$p_1(x) = x[0.0164609x^2 + x(-0.0617284 + 0.123457y - 0.0740741y^2) + 1.44444(0.743784 - 1.71357y + y^2) \times (0.287281 - 1.00438y + y^2)]$$

$$q_1(x) = (0.833333 - y)^4 \quad (47)$$

Alternatively, the indefinite integral in the y -direction yields

$$\int 3b_{11}^2 + b_{31}^2 dy = -\frac{p_2(x, y)}{q_1(x, y)},$$

where

Table 1. Integrated Strain Energy Densities: Stiffness Matrix of Trapezoid

0.861515	0.3931	-0.361515	0.1069	-0.553939	-0.427599	0.0539388	-0.0724008
0.3931	0.874149	0.1069	0.625851	-0.427599	-0.503403	-0.0724008	-0.996597
-0.361515	0.1069	1.11152	-0.6069	0.0539388	-0.0724008	-0.803939	0.572401
0.1069	0.625851	-0.6069	1.62415	-0.0724008	-0.996597	0.572401	-1.2534
-0.553939	-0.427599	0.0539388	-0.0724008	1.78424	0.289603	-1.28424	0.210397
-0.427599	-0.503403	-0.0724008	-0.996597	0.289603	1.98639	0.210397	-0.486388
0.0539388	-0.0724008	-0.803939	0.572401	-1.28424	0.210397	2.03424	-0.710397
-0.0724008	-0.996597	0.572401	-1.2534	0.210397	-0.486388	-0.710397	2.73639

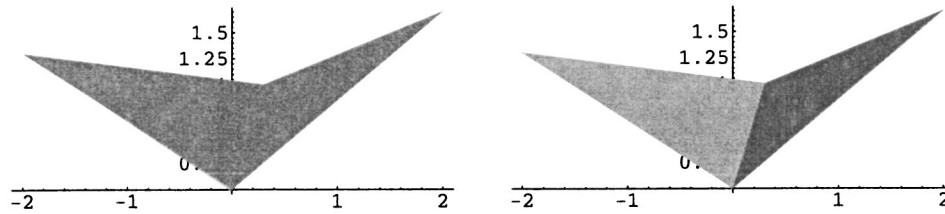


Fig. 6. Concave element—composed of two triangles

$$\begin{aligned}
 p_2(x,y) = & -0.10419 + 0.0914495x - 0.0137174x^2 - 0.322931y \\
 & - 0.315501xy + 0.0164609x^2y + 2.89609y^2 \\
 & + 0.37037xy^2 - 5.83951y^3 - 0.148148xy^3 + 4.81481y^4 \\
 & - 1.44444y^5 - (0.428669 - 2.05761y + 3.7037y^2 \\
 & - 2.96296y^3 + 0.888889y^4) \log(0.833333 - y) \quad (48)
 \end{aligned}$$

The indefinite integral in Eq. (47) could differ by a function in y in another symbolic integration computer program. This is of no concern [see Eq. (17b)], for the net contribution of this arbitrary function will be zero. The argument holds for the indefinite integral in Eq. (48).

Concave Element

The proposed integration scheme is not restricted to convex elements. This has been established analytically with illustrations (Fig. 2). Many integration schemes yield numerical errors when a reentrant corner is encountered at a node of concavity. The following examples assure an analyst that the symbolic algebra computer code presented in Appendix II can be safely used when integration within concave polygons are needed.

In Fig. 6, two triangles with the following coordinates—

$$\text{left triangle } \Omega_1: (0,0), (0,3,1), (-2,1,3) \quad (49a)$$

$$\text{left triangle } \Omega_2: (0,0), (0,3,1), (2,1,7) \quad (49b)$$

—are “glued” along the common side to create a concave region:

$$\text{concave quadrilateral } \Omega^*: (0,0), (2,1,7), (0,3,1), (-2,1,3) \quad (50)$$

The *Mathematica* code of Appendix II has been used to evaluate integrals of a function:

$$z = z(x,y) \quad (51)$$

as

$$I_1 = \int_{\Omega_1} z dA; \quad I_2 = \int_{\Omega_2} z dA; \quad I^* = \int_{\Omega^*} z dA; \quad (52)$$

The relative error \mathcal{E} is computed to be

$$\mathcal{E} = 1 - \frac{I_1 + I_2}{I^*} \quad (53)$$

The results are presented in Table 2.

The results are satisfactory with the fifth-order Gaussian quadrature. There is no noticeable error in the following cases:

Example 1: $z = 1$: Checks the area calculations

Example 2: $z = y$: Used in determining the centroid

Example 3: $z = y^2$: Needed to calculate second moments of the area

Example 4: $z = y \exp(-y)x^4$: This function is chosen arbitrarily.

Example 5: $z = \sqrt{y}$: The finite-element shape functions for triangles with side nodes involve square roots (Wachspress 1975). The accuracy is tested here for such an irrational function.

Example 6: $z = \sin(y)$: An oscillatory function is tested.

Conclusions

The applicability of Gaussian quadrature, which is the most popular numerical integration procedure, is extended in this presentation to two- and three-dimensional arbitrarily shaped domains that are bounded by straight lines and planes, respectively. Similar $(n-1)$ repeated applications of the divergence theorem can convert an n -dimensional domain integral within a polytope in \mathcal{R}^n into a set of one-dimensional integrals that can be conveniently evaluated by an available Gaussian quadrature computer program.

At each stage of the application of the divergence theorem, an indefinite integral must be evaluated. The significant development in the computer algebra software and its wide availability empower an analyst to combine analytical evaluation of integrals in different single variables with a numerical implementation of Gaussian quadrature.

Historically, requirements in the aerospace technology and bioengineering (McAlarney et al. 1991) motivated the development of high-accuracy algorithms in computational mechanics. When secondary effects, e.g., material randomness and geometrical imperfections, need to be addressed, unconventional special purpose computer programs become indispensable in order to embed uncertainty in the basic test functions and to implement energy density integration algorithms that faithfully preserve the preassigned numerical tolerance (Dasgupta 1989; Vilmann and Dasgupta 1992). The paper addresses the latter issue with long-hand examples.

The divergence theorem plays the key role in transforming a domain integral in \mathcal{R}^n into an equivalent boundary integral in \mathcal{R}^{n-1} . After successive reduction of the spatial variables, the one-dimensional Gaussian quadrature can finally be implemented. The major assumption here is that the boundary of the finite domain in

Table 2. Comparison of Numerical Results on Concave Element

Case	Function	I_1	I_2	I^*	\mathcal{E}
I	1	1.195	0.745	1.94	0
II	y	0.916167	0.6705	1.58667	0
III	y^2	0.794675	0.694092	1.48877	0
IV	$y \exp(-y)x^4$	0.401535	0.32334	0.724875	0
V	\sqrt{y}	1.02447	0.690525	1.71499	0
VI	$\sin(y)$	0.798837	0.549467	1.3483	0

Table 3. Quadrature Points and Weights: Fifth-Order Scheme

Point	0.0469101	0.230765	0.5	0.769235	0.95309
Weight	0.118463	0.239314	0.284444	0.239314	0.118463

\mathfrak{R}^n is approximated by linear manifolds of \mathfrak{R}^{n-1} , which are generalized planes described by linear combinations of variables in $n-1$ dimensions. For an integrand, a function is sought whose total derivative would be that integrand. An important theoretical question emerges regarding the effects of the accompanying arbitrary constants that appear during the implementation of the divergence theorem. Analytical proofs demonstrating the zero effect of such arbitrary terms during indefinite integrations in two- and three-dimensions established the applicability of the proposed method. Its generalization in \mathfrak{R}^n is evident.

It is anticipated that, in stochastic finite elements and stochastic boundary elements, the proposed integration scheme will be implemented to yield more reliable aerodynamic responses. Probability integrals to predict extreme occurrences and exceedences are closely related to the β - and Γ - functions (Gumbel 1958). These can be computed with a desired numerical precision for predicting behavior of aircraft components that have unconventional shapes. An illustrative example is included in this paper.

Difficulties in numerical integration of energy density functions have been a major deterrent in using polygons and polyhedra of large numbers of sides and faces, respectively, in finite-element calculations. Such hindrances are conceptually removed here to yield more accurate discretizations beyond Courant's linear (Courant 1943) and Taig's (Taig 1961) isoparametric formulations.

Acknowledgment

The research was funded by the National Science Foundation, Grant No. CMS 9820353. Support of COBASE-NRC and Fulbright Foundation, USA, is gratefully acknowledged. This paper is dedicated to the memory of the Late Professor Bimalendu Sen, former Principal of Bengal Engineering College, Howrah, West Bengal, India.

Appendix I. Gaussian Quadrature

To facilitate code development, sample Gaussian quadrature results are summarized here. Table 3 is used. These sampling points and weights are used in the *Mathematica* calculations presented in Table 2.

The following integral expressed as an n -order quadrature—

$$\int_a^b f(\xi) d\xi = \sum_{i=1}^n w_i f(\xi_i) \quad (54)$$

—is stated in the nondimensional form, where $a=0$ and $b=1$. For each sampling point x_i ,

$$x = \frac{\xi - a}{b - a}; \quad \int_0^1 f(x) dx = \sum_{i=1}^n w_i f(x_i) \quad (55)$$

Standard quadrature packages use the fifth-order rule since it achieves adequate accuracy for most of the finite-element problems.

To illustrate the use of Table 3 the following example is presented:

$$\int_0^1 x \sin(x) dx = \sin(x) - x \cos(x) \Big|_0^1 = 0.301169 \quad (56)$$

For $n=5$ the sampling points are 0.0469101, 0.230765, 0.5, 0.769235, and 0.95309. The last two points are calculated by subtracting the second and the first values from one. The observed values of $x \sin(x)$ are 0.00219975, 0.0527813, 0.239713, 0.535069, and 0.776967.

The respective weights are 0.118463, 0.239314, 0.284444, 0.239314, and 0.118463.

The fourth and the fifth weights are identical with the second and the first, respectively.

Sum of the multiplication of weights and the sampled values:

$$\begin{aligned} &0.00219975 \times 0.118463 + 0.0527813 \times 0.239314 + 0.239713 \\ &\times 0.284444 + 0.535069 \times 0.239314 + 0.776967 \times 0.118463 \\ &= 0.301169. \end{aligned}$$

The final value is the same as the result in Eq. (56).

Appendix II. Mathematica Code

```
AreaIntegrate::usage='AreaIntegrate[z, {x, y}, nodes]
yields the numerical value of z, a function of {x, y}
coordinates, integrated within nodes.'
```

```
IntegrateApart [x_, t_Symbol] :=Module[{z},
z=Apart [x, t];
```

```
If [Head[z] ===Plus,
Plus@@Map[Integrate[#, t]&, List@@z],
Plus@@Map[Integrate[#, t]&, Replace[z,
Plus[y_] ->List [y]] ] ]
```

```
IntegrateApart[x_, {t_Symbol, t1_, t2_}] :=(
(#/.t->t2) -(#/.t->t1))&[
IntegrateApart [x, t]]
```

```
AreaIntegrate[z_, {x_, y_}, nodes_] :=Module[
{zx, t, segments},
zx =IntegrateApart[z, x];
segments =Partition[Append[nodes,nodes [[1]]], 2, 1]
Plus@@Map[LineIntegrate[zx, {x, y, t}, #]&,
segments]]
```

```
LineIntegrate [z_, {x_, y_,t_}, {{x1_, y1_}, {x2_, y2_}}]:=
(IntegrateApart[
((y2 -y1) z)/.{x->x1 +t(x2 -x1),y->y1 +t(y2 -y1)},
{t, 0, 1}])
```

References

- Aleksandrov, P. S. (1960). *Combinatorial topology*, Dover, Albany, N.Y.
- Bathe, K. J. (1996). *Finite element procedures*, 4th Ed., Prentice-Hall, Englewood Cliffs, N.J.
- Courant, R. (1943). "Variational methods for the solution of problems of equilibrium and vibration." *Bull. Am. Math. Soc.*, 49, 1–29.
- Dasgupta, G. (1989). "Boundary elements with macro shape functions." *Advances in boundary elements*, C. Brebbia and J. Connor, eds., Computational Mechanics Publications, Ashurst, Southampton, U.K., 253–262.
- Dasgupta, G. (1992). "Approximate dynamic responses in random media." *Acta Mech.*, 3, 99–114.
- Dasgupta, G. (2000). "Successful patch tests for wachspres elements." *Rep. April 2000, CEEM-GD-2000-2*, Columbia University, New York.
- de Berg, M., van Kreveld, M., Overmars, M., and Schwarzkopf, O. (2000). *Computational geometry: Algorithms and applications*, 2nd Ed., Springer, Berlin.
- Gumbel, E. J. (1958). *Statistics of extremes*, Columbia University Press, New York.

- Hughes, T. J. R. (1987). *The finite element method*, Prentice-Hall, Englewood Cliffs, N.J.
- Irons, B. M., and Razzaque, A. (1972). *Experience with the patch test for convergence of finite elements method*, Academic Press, New York.
- Keller, J. B. (1964). *Stochastic Equations and Wave Propagation in Random Media, Proc., Symposium on Applied Mathematics*, Vol. 16 American Mathematical Society, Providence, R.I.
- Keller, J. B., and McKean, H. P. (1973). "Siam-ams proceedings." *Stochastic differential equations*, Vol. VI, American Mathematical Society, Providence, R.I.
- MacNeal, R. H. (1994). *Finite elements: Their design and performance*, Marcel Dekker, New York.
- McAlarney, M. E., Dasgupta, G., Moss, M. L., and Moss-Salentijn, L. (1991). "Boundary macroelements and finite elements in biological morphometrics: A preliminary comparison." *Computers in biomedicine*, K. D. Held, C. A. Brebbia, and R. D. Ciskowski, eds., Computational Mechanics Publisher, Southampton, U.K. 61–72.
- Molyneux, J. E. (1968). "Analysis of 'dishonest' methods in the theory of wave propagation in a random medium." *J. Opt. Soc. Am.*, 58, 951–957.
- Reddy, J. N. (1984). *An introduction to the finite element method*, McGraw-Hill, New York.
- Rogers, D. F., and Adams, J. A. (1990). *Mathematical Elements of Computer Graphics*, McGraw-Hill, New York.
- Strang, G., and Fix, G. J. (1973). *An analysis of the finite element method*, Prentice-Hall, Englewood Cliffs, N.J.
- Taig, I. C. (1961). "Structural analysis by the matrix displacement method." *Rep. S017*, English Electric Aviation Report, England.
- Vilmann, O., and Dasgupta, G. (1992). "Fundamental solutions for stochastic mindlin plates." *Int. J. Eng. Anal.*, 9, 47–59.
- Wachspress, E. L. (1971). *A rational basis for function approximation*, Vol. 228 of *Lecture Notes in Mathematics*, Springer Verlag, Berlin.
- Wachspress, E. L. (1975). *A rational finite element basis*, Academic, San Diego.
- Wolfram, S. (1997). *The Mathematica book*. Cambridge University Press, New York.
- Zienkiewicz, O. C., and Taylor, R. L. (2000). *The finite element method*, Vol. 1, 5th Ed., Butterworth, Heinemann, Elsevier Science, Burlington, Mass.